Supplementary Information

Intense and repeatable orange mechanoluminescence of Mn^{2+} activated $CaGa_4O_7$ for visualized mechanics sensing

Yongwen He,[a,b] Jie Wang,[c] Shaofan Fang,[d*] Junshan Qin,[e] Long Feng,[d] Birong Tian,[a,d] Shaowei Feng,[c*] and Zhaofeng Wang,[a,b,d *]

[a] *State Key Laboratory of Solid Lubrication, Lanzhou Institute of Chemical Physics, Chinese Academy of Sciences, Lanzhou, Gansu 730000, China*

[b] *Center of Materials Science and Optoelectronics Engineering, University of Chinese Academy of Sciences, Beijing 100049, China*

[c] *Beijing Institute of Astronautical Systems Engineering, Beijing 100076, China*

[d] *Shandong Laboratory of Advanced Materials and Green Manufacturing at Yantai, Yantai, Shandong 265503, China*

[e] *Jiuquan Iron & Steel Group Co. Ltd., Jiayuguan, Gansu 620200, China*

[*]Authors to whom correspondence should be addressed:

Dr. Zhaofeng Wang, Tel: +86-931-4968682; Email: zhfwang@licp.cas.cn (Z. Wang)

Dr. Shaofan Fang, Email: sffang@amgm.ac.cn (S. Fang)

Dr. Shaowei Feng, Email: fawwi@126.com (S. Feng)

1. Structure and Morphology

Table S1. Structural refinement parameters of CGOM: Crystal data of refined sample.

Chemical formula	$CaGa_4O_7$				
Crystal system	monoclinic				
Space group	*C*2/*c* (No.15)				
Z	4				
X-ray diffractometer	Rigaku D/max-240				
Temperature	298 K				
Theta range for data collection	10° to 80°				
Mn^{2+} concentration (%)	**0.025**	**0.05**	**0.1**	**0.2**	**0.3**
a (Å)	13.118	13.118	13.118	13.117	13.117
b (Å)	9.114	9.113	9.113	9.113	9.112
c (Å)	5.610	5.610	5.609	5.609	5.609
V ($Å^3$)	647.736	647.638	647.591	647.419	647.364

Table S2. Structural refinement parameters of CGOM: Refined coordinates of all atoms.

Atom	**Ion coordinates**			**Occupancy**	**Uiso**
	x	**y**	**z**		
Ca	0.00000(0)	0.29479(0)	0.25000(0)	1.00000(0)	-0.00230
Ga1	0.12076(0)	0.06234(0)	0.74350(0)	1.00000(0)	0.00945
Ga2	0.33995(0)	0.08739(0)	0.18540(0)	1.00000(0)	0.00799
O1	0.19386(0)	0.06016(0)	0.08360(0)	1.00000(0)	0.02533
O2	0.38611(0)	0.06918(0)	-0.09620(0)	1.00000(0)	0.01313
O3	0.11302(0)	0.26684(0)	-0.36711(0)	1.00000(0)	0.03074
O4	0.00000(0)	0.03486(0)	0.25000(0)	1.00000(0)	0.04165

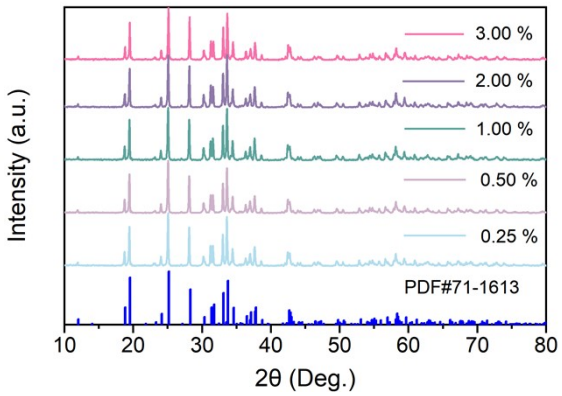

Figure S1. XRD patterns of CGOM with different Mn^{2+} doping concentrations synthesized at 1473 K for 6 h.

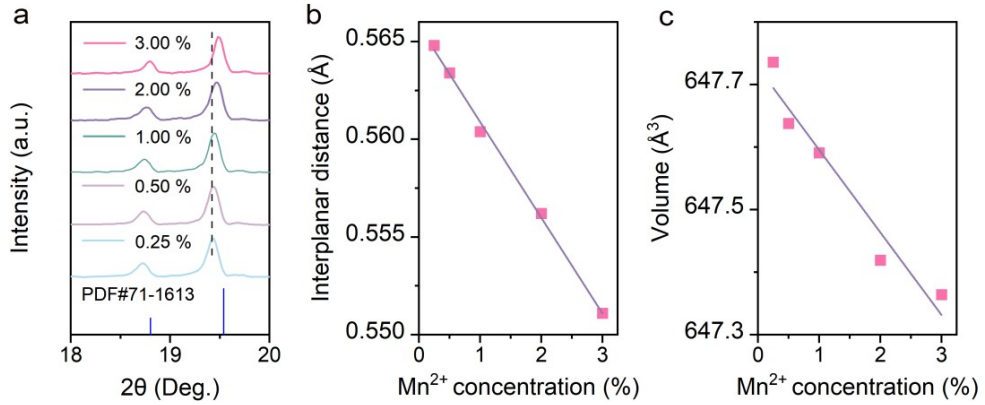

Figure S2. a) Partially enlarged image for XRD patterns. b) Interplanar distance of (020) as a function of Mn^{2+} concentration. c) Cell volume as a function of Mn^{2+} concentration.

It can be seen from Figure S1 that all the diffraction peaks of the samples with different Mn^{2+} doping concentrations can be well indexed to the standard card (PDF#71-1613). Moreover, we investigated the peak shifts by amplifying the diffraction peak at 25°, and calculated the values of cell volume. Due to the smaller ion radius of Mn^{2+} than Ca^{2+}, the diffraction peak gradually shifts to the large angle with the increase of the Mn^{2+} doping concentration from 0.25% to 3%, as shown in Figure S2a-b. Meanwhile, Figure S2c show that the cell volume decreases linearly with the increase of the Mn^{2+} doping contents. These results in terms of the peak shifts and cell volume changes confirm that Mn^{2+} has been successfully doped in $CaGa_4O_7$.

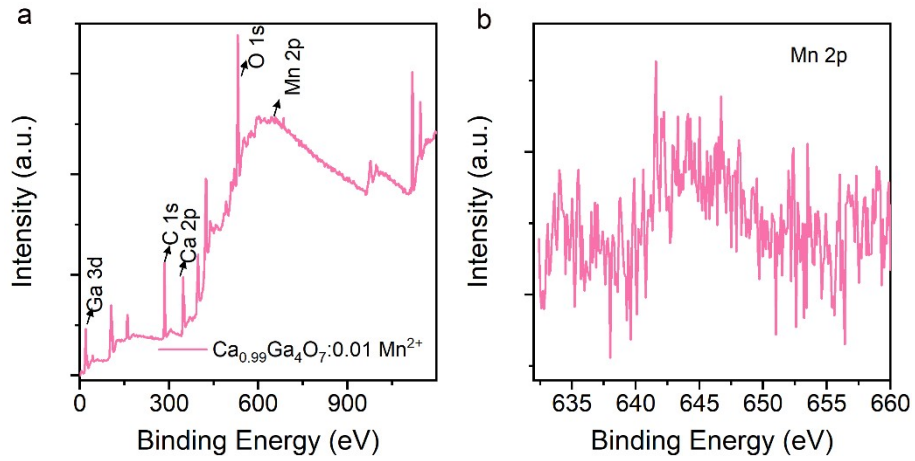

Figure S3. a) XPS survey spectra and b) high-resolution Mn 2p XPS spectrum of CGOM.

The XPS survey spectrum in Figure S3a suggest that the Mn ions exist in CGOM. The high-resolution XPS spectrum of Mn 2p (Figure S2b) confirms that the valence of Mn cations is +2 after sintering in a strong reducing atmosphere (90% N_2 and 10% H_2).

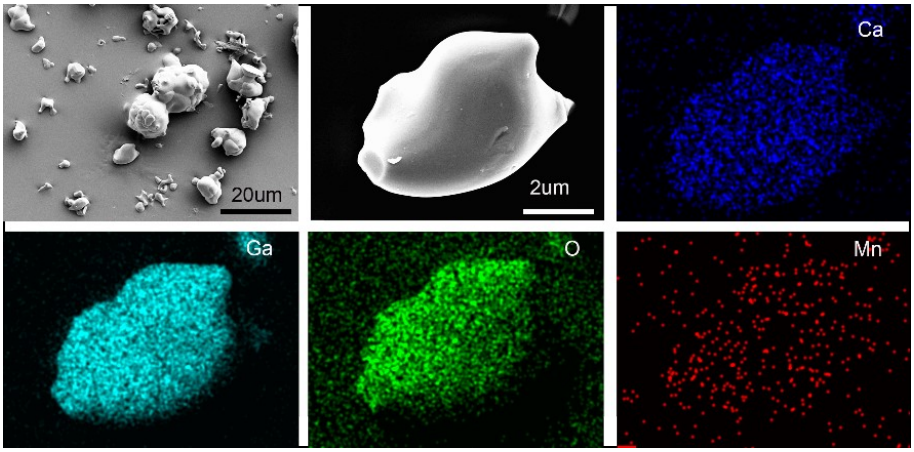

Figure S4. SEM image and EDS mappings of the CGOM powders.

As presented in Figure S4, the SEM images disclose the morphology and microstructure of CGOM powders. The particles show irregular shape and relatively smooth surfaces with the size range from 4 to 20 μm. The EDS mappings validate that Ca, Ga, O, and Mn have been distributed in the powders.

2. ML and Mechanical Performance

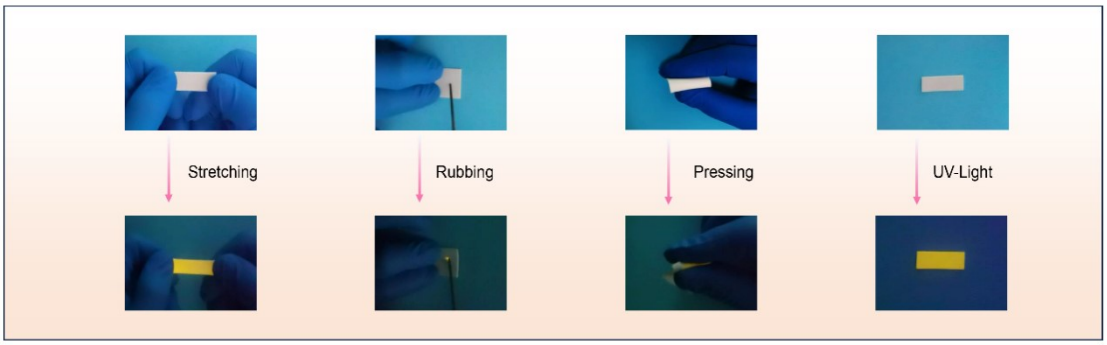

Figure S5. Photographs of the CGOM/PDMS composite film under UV light or different mechanical stimulations.

It can be seen from Figure S5 that the emission light of the CGOM/PDMS film under UV light and stretching, rubbing, pressing can be facilely captured by the naked eye and cameras even in the bright environment.

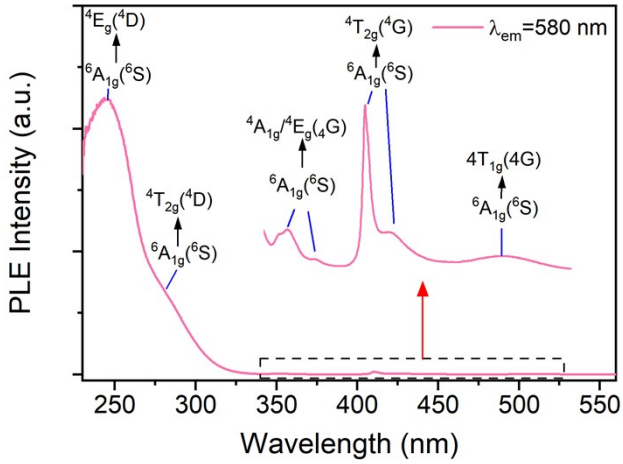

Figure S6. Photoluminescence excitation spectrum of CGOM monitored at 580 nm.

When monitored at 580 nm, the CGOM exhibits a broad excitation band attributing to the charge transfer band and $^6A_{1g}(^6S) \rightarrow {}^4E_g(^4D)$ transition. In addition, several weak excitation peaks are found at 289, 354/373, 413/428, 509 nm, attributing to the $^6A_{1g}(^6S) \rightarrow {}^4T_{2g}(^4D)$, $^6A_{1g}(^6S) \rightarrow {}^4A_{1g}/{}^4E_g(^4G)$, $_6A_{1g}(^6S) \rightarrow {}^4T_{2g}(^4G)$, $^6A_{1g}(^6S) \rightarrow {}^4T_{1g}(^4G)$ transitions of Mn^{2+}, respectively.

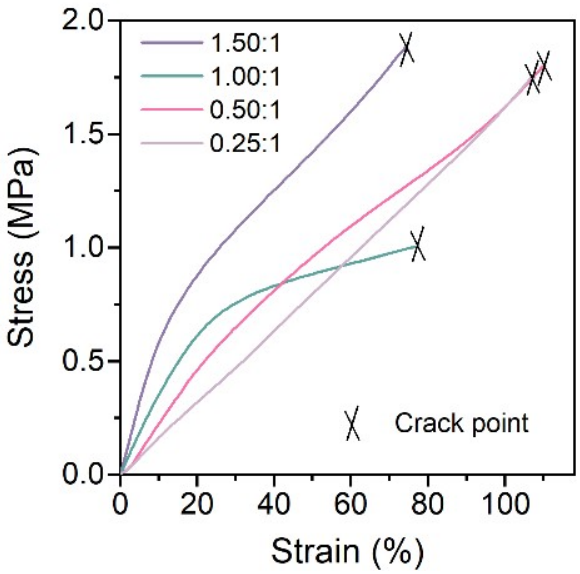

Figure S7. Stress-strain curves of the CGOM/PDMS composite elastomers under different powder-gel ratio.

It can be observed from Figure S7 that with the increase of the powder-gel ratio, the elastic modulus of the composite elastomer rises, and the fracture point is advanced. Moreover, the stress-strain curve deviates from the linear relationship when the powder-gel ratio is large. Therefore, a large powder-gel ratio will lead to poor flexibility of CGOM/PDMS composite elastomers, which is not conducive to the mechanical sensing applications.

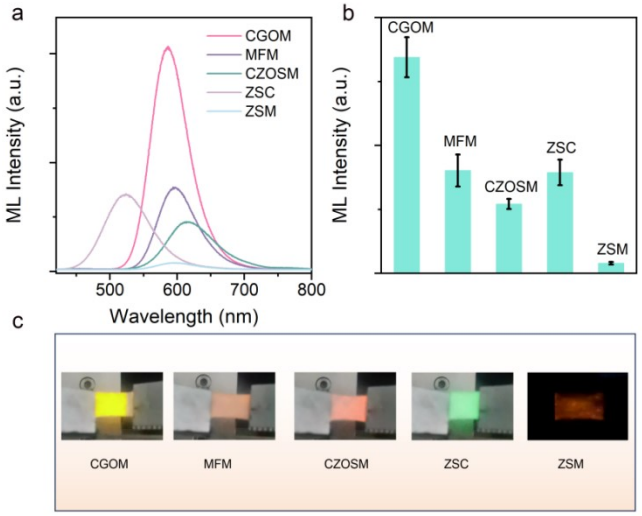

Figure S8. a) ML spectra, b) ML intensity comparison, and c) ML photographs of the CGOM and other ML samples ($CaGa_4O_7$:Mn (CGOM), MgF:Mn (MFM), CaZnOS:Mn (CZOSM),

ZnS:Cu (ZSC), ZnS:Mn (ZSM)) composited into PDMS under the same stretching conditions (stain: 60%; frequency: 3 Hz).

It can be observed from Figure S8 that the ML intensity of the CGOM/PDMS sample is conspicuously higher than that of other samples during the initial stretch.

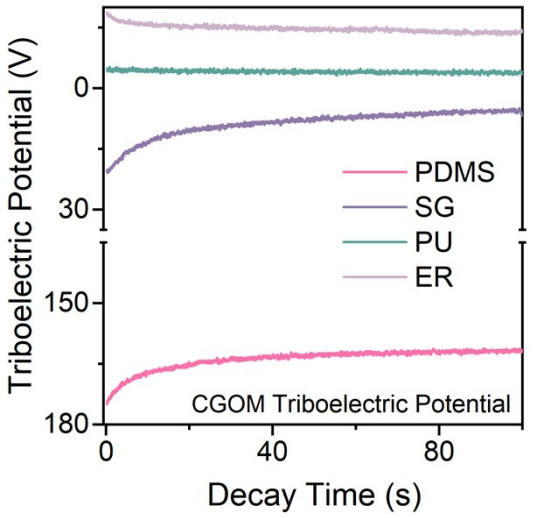

Figure S9. Attenuation curves of CGOM after rubbing with PDMS, SG, PU, ER for 1 min.

3. EL test

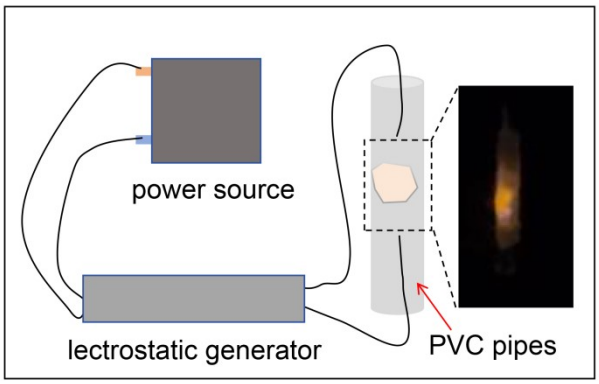

Figure S10. The electrostatic generator (JD01-1230) stimulated light of the CGOM.

The CGOM powders were put in the middle of a PVC pipe first. An electrostatic generator with an output voltage of 30 kV was employed to generate the electric field, and the positive and negative electrodes were fixed at both ends of the pipe. The CGOM powders were directly excited by the electric field. After powering on, the CGOM

powders were observed to emit orange light.

4. Potential Applications

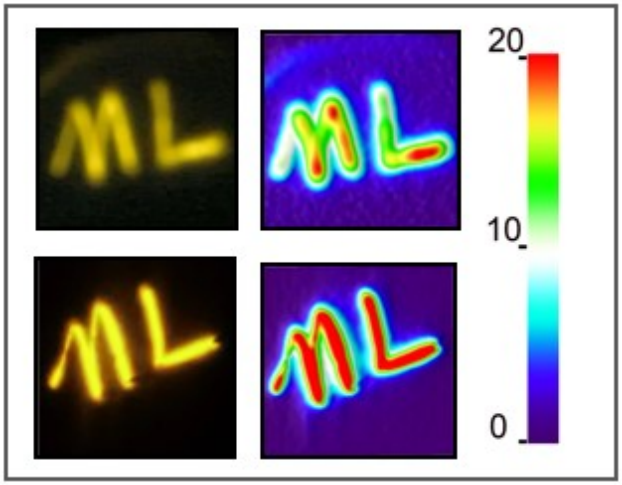

Figure S11. Handwriting identification based on the ML of CGOM/PDMS composite film.

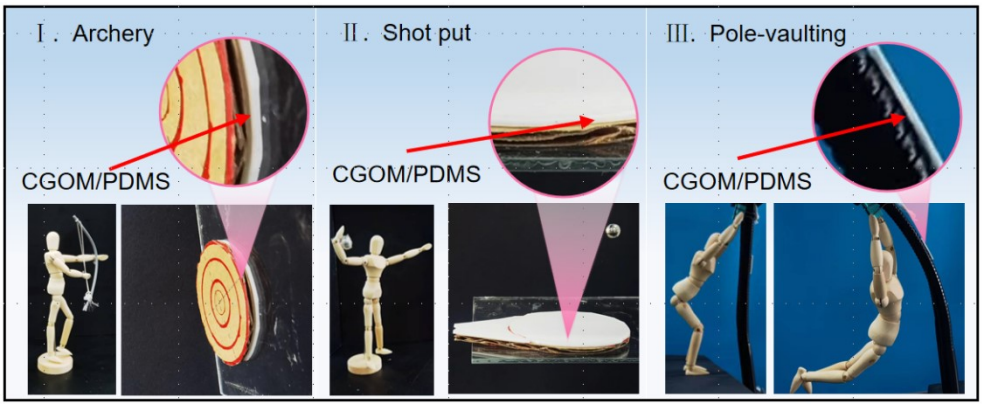

Figure S12. Visualization of the mechanical information in competitive sports: I) target material in archery, II) landing area of shot put, and III) pole in pole vault.